

Physics of Separated Flows – Numerical, Experimental, and Theoretical Aspects

DFG Priority Research Programme
1984–1990

Edited by
Klaus Gersten

Notes on Numerical Fluid Mechanics, Volume 40
(Vieweg, Braunschweig 1993)

The title of the book series is allowed to be abbreviated as NNFM.



Reprint

EXPERIMENTAL INVESTIGATION OF LAMINAR SEPARATION BUBBLES

D.Althaus and W.Würz
Institut für Aerodynamik und Gasdynamik, Universität Stuttgart

INTRODUCTION

Laminar separation bubbles play an important role in the flow about airfoils at Reynolds numbers below 3 millions in incompressible flows. Drag as well as stall behaviour can be deteriorated considerably. Designing or analysing airfoils in this flight regime, with some success, requires understanding of the flow phenomena involved in the formation of these regions with locally separated flow. Detailed experimental studies were carried out on laminar separation bubbles that formed near the midchord of different airfoils at Reynolds numbers from 0.7 to 3 millions. Static pressure, hot wire anemometry, and flow visualisation data were acquired. The data were used to evaluate the applicability of existing separation bubble models. Some details of the materials gathered are presented in the following context.

WIND TUNNEL

The Laminar Wind Tunnel of the Institute (Fig.1) is built as an open return tunnel of the Eiffel design [1]. The high contraction ratio of 100:1 and the screens result in a very low turbulence level of less than $2 \cdot 10^{-4}$. The rectangular test section measures 0.73m * 2.73 m and is 3.15 m long. The two dimensional airfoil models span the short distance of the test section. The gaps between the model and the tunnel walls are sealed. Blowing air tangential in the corner between the model and the mounting plates is used as a boundary layer control to ensure two-dimensional conditions.

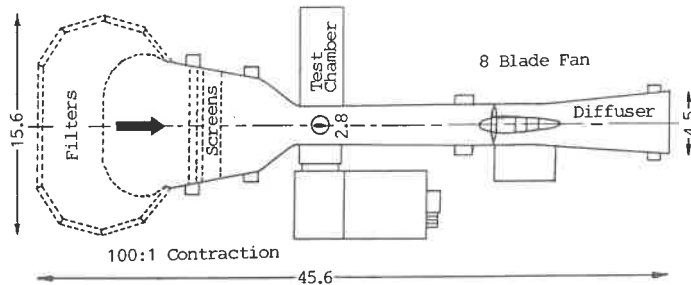


Fig.1: Laminar Wind Tunnel (dimensions in meters)

INSTRUMENTATION AND PROCEDURE

The boundary layers over the airfoils were surveyed by a Disa hot wire anemometry system in constant-temperature mode with a Disa type 55P15 single wire boundary-layer probe. The static

pressure distribution was obtained by using a static pressure tube of 1mm diameter with its bores at the same streamwise location as the hot-wire but 20mm apart. The probes are mounted to a small traversing mechanism (Fig.2b). A thin support resting on the airfoil surface defines its position in relation to the wall. By means of a high precision rack- and pinion drive together with an optical encoder a resolution of $5\mu\text{m}$ in wall distance is achieved. To enable boundary layer traverses vertical to the airfoil surface this unit can be tilted about its sting (Fig.2a), which itself can be positioned at any station on the airfoil by remotely controlled DC-motors. The surface of the airfoils is coated with a thin layer of graphite-spray which makes it electrically conductive. To start traversing a boundary layer, the hotwire probe is moved towards the wall until its prongs touch the graphite thus closing an electric circuit with high impedance which stops the motor. The direction of traverse is then reversed and the probe moves until its contact with the wall breaks. By this means eventual backlash and bending effects are removed. This position is taken as the zero wall distance.

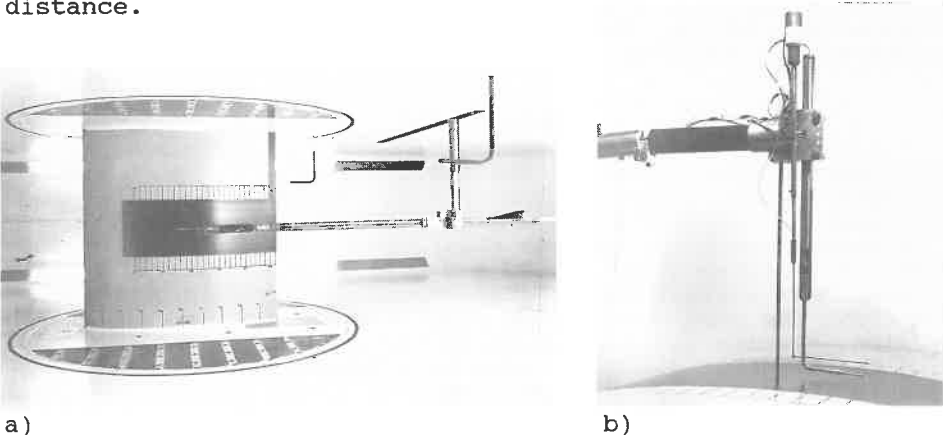


Fig.2: Traversing mechanism for boundary layer measurements

The output of the hotwire anemometer unit is fed to a Disa 55D10 Linearizer. The mean velocity component is integrated by a low pass filter at 1. or .5 Hz. The fluctuating component is measured by a Disa 55D35 true-rms-meter. The outputs of these instruments including the voltages proportional to wall distance, tunnel speed and static pressure are sampled by a 12-bit analog to digital converter connected to a PDP 11/34 computer. Moving of the probe, delay time for settling of the instruments and sampling of the data are controlled by the computer in a cyclic manner. Mean velocity and fluctuating velocity are immediately plotted in relation to wall distance as a boundary layer profile. In addition the hot-wire signal is watched on an oscilloscope. Thirty to sixty points are acquired in each of the profiles. The locations of these stations were chosen according to the position of the separation bubbles. For FFT-analysis the fluctuating portion of the hot-wire signal is amplified and low-pass filtered according to the

sampling rate. Normally, the filter is set to 5 KHz at a data rate of 10 KHz. Typical Tollmien-Schlichting frequencies at test conditions are in the order of 1 kHz. At several points of a station spectral data were preferably acquired at the position of maximum turbulence energy. Up to 4096 data points were sampled by a 12-bit a-d converter connected to a PC-80486 computer. The spectral data could be immediately inspected on the monitor, thus enabling to adjust the amplification of the signal.

DISCUSSION OF RESULTS

Length and thickness of separation bubbles depend on the pressure distribution of the outer flow and the conditions in the separation point. With growing Reynolds number and/or growing angle of attack both dimensions are reduced in mid-chord bubbles. The streamline which divides the "dead-air" region and the separated laminar shear layer prevents the exchange of flow between the regions. To find its position above the wall a heating wire with a diameter of 0.1mm and 200mm in length was placed parallel and close to the wall and vertical to flow direction within the "laminar part" of the bubble. This wire was periodically heated by an electric pulse. A temperature probe instead of a hot-wire is attached to the traversing mechanism and moved stepwise away from the wall. As long as this probe moves within the bubble it records the temperature pulses. They are recorded by a flashing light or by the oscilloscope. When the separating streamline is reached the pulses disappear. The height of the dividing streamline ψ is marked (s. Fig.8) in the boundary layer profile (acquired with the hot-wire) together with the position of the line $u=0$, which is at $2/3 \psi$ [2]. By repeating this procedure at different stations downstream of the separation, the contour of the streamline can be recorded. As the position of the line $u=0$ is close to the height where the hot-wire begins to read $u>0$ and where the fluctuating velocity grows it is normally found by interactive computer graphics. The evaluation of the streamline data showed that they are nearly straight lines which are slightly bended upward when plotted over a straight axis (Fig.3 $u=0$ line). Its height, however, was measured from the airfoil surface, which has a curvature. Fig.4 shows the contour of the bubble $u=0$ line plotted over the airfoil shape. In Figure 5 the tangent of the separation angle of the line $u=0$ multiplied with the Reynolds number Re_{δ_2} based on conditions at separation, is plotted over $m_{s \rightarrow p}$ which uses the derivative of the velocity distribution and the momentum thickness at separation. The circles represent different test series by their numbers. Dobbinga

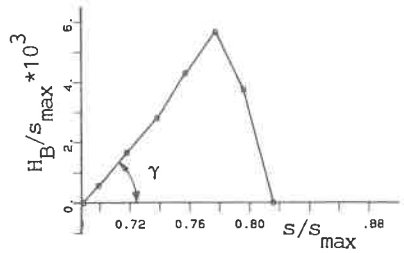


Fig.3: Bubble contour

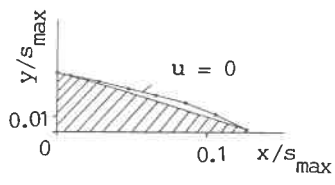


Fig.4: Bubble contour over airfoil shape

et al. [2] found that $B = \tan \gamma * Re_{\delta_{2sep}} = \text{const} = 15 - 20$.
 The dotted line corresponds to

$$B = \tan \gamma * Re_{\delta_{2sep}} = 2.7 + 416.7 * m_{sep}^2$$

and is a reasonable good approach. Wortmann proposed $B = 64 * P$, where P is based on the gradient $\Delta u / \Delta s$ between separation and recovery. But the point of recovery is not known at the very beginning.

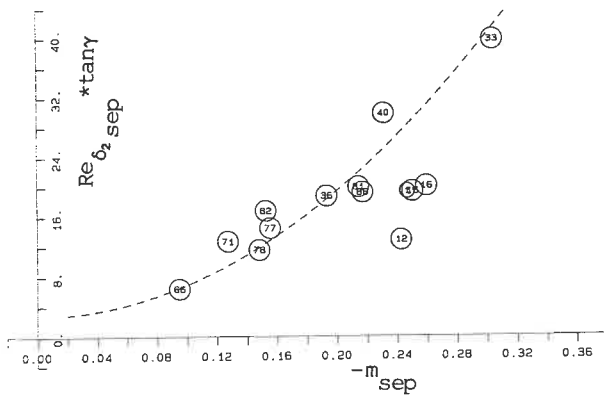


Fig.5: Separation angle γ for different measurements

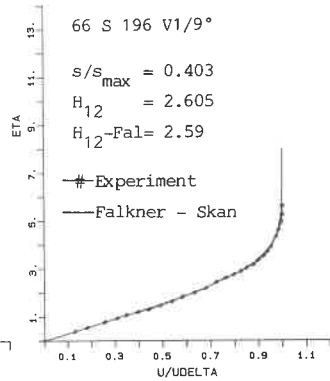


Fig.6: Laminar boundary layer profile

Boundary layer conditions at separation are essential for modelling the separation bubbles. The velocity at the edge of the boundary layer, however, is modified by the bubble. Therefore it can not be used for a model. With this background the separation bubble is removed by a surface-roughness which causes transition just before the separation point. A new velocity distribution is acquired along the region of the bubble (Fig.10). This is used for boundary layer calculations and in modelling the bubble.

Comparisons are made between experimental and theoretical velocity profiles in the boundary layer. Fig.6 shows experimental data points together with a profile of the similar Falkner-Skan family with equal shape parameter H_{12} . The good correlation is a proof for the quality of the velocity and wall-distance data. When separation is approached however experimental profiles no longer conform to Falkner-Skan profiles (see Fig.7a). Fig. 7b shows that this profile can be matched by a function due to Liu and Sandborn [3]. In Figs.6 and 7a the wall distance is normalized by η .

The experimental profiles within the "dead air" region show zero velocity below the $u=0$ position (s.Fig.8) down to streamwise stations a short distance before the maximum bubble height is reached where fluctuating and mean velocity begin to grow when transition begins (Fig.9). For computing amplification rates by the Orr-Sommerfeld equation and for modelling the bubble velocity profiles in analytical form are required. In Fig. 8a it is attempted to approximate an experimental boundary-layer profile by a profile of the Falkner-Skan family which affords backflow in the wall region. The hot-wire is unable to distinguish the tangential velocity from the normal one and from reverse flow, but in Fig. 8 it shows no

flow at all. A Green profile [4] which is composed of a part with constant velocity in the wall region and a Coles wake-profile is a very good approximation as Fig. 8b shows. In Fig. 9a the hot wire measures small and constant velocity below the $u=0$ position. The Falkner-Skan profile affords higher reverse flow than the Green profile in Fig.9b. An experimental profile in the turbulent part of the bubble can be approximated by a Green profile with or without backflow.

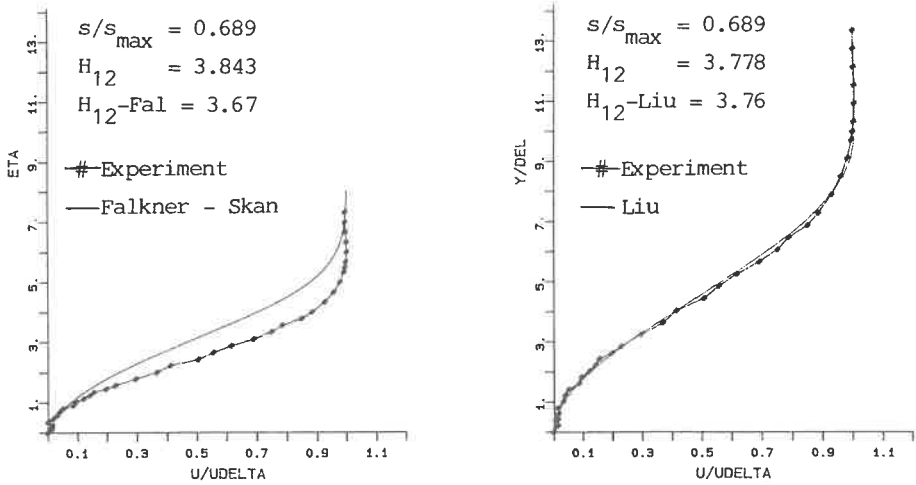


Fig.7: a) Experimental and Falkner-Skan Profile at Separation
b) Separation Profile from Liu and Sandborn

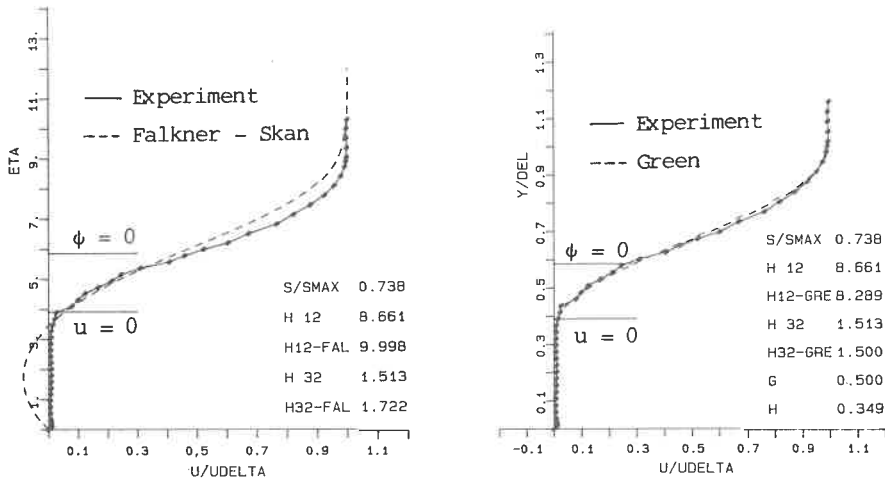


Fig.8: a) Exp. and Falkner-Skan Profile in separated region
b) Exp. and Green Profile in separated region

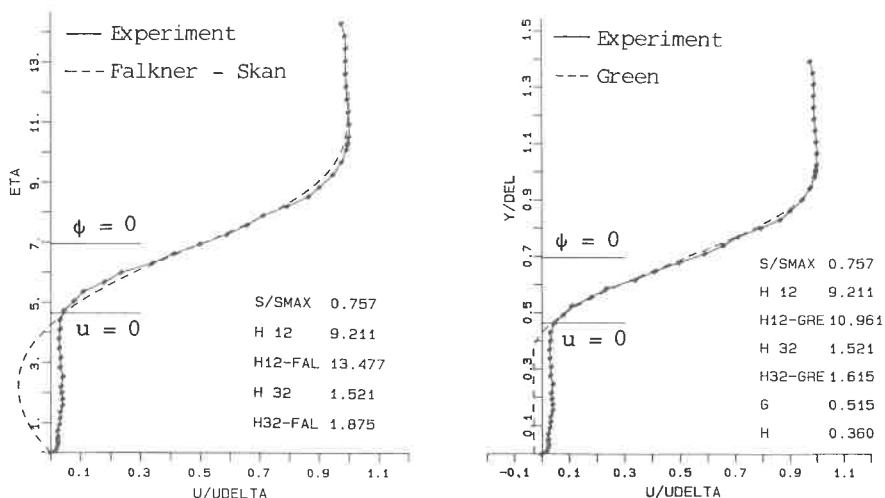


Fig.9: Exp. and analytical profiles in the separated region
 a) Falkner-Skan
 b) Green

Hot-wire results are reliable in the laminar part of a laminar separation bubble. Green profiles yield better approximations to experimental points than Falkner-Skan profiles. This is also confirmed by Fitzgerald and Mueller [5] who make comparisons with Laser Doppler Anemometer measurements at low Reynolds numbers.

Fig. 10 shows the differences between a boundary layer with a separation bubble and a boundary layer in which transition is tripped just before the separation point (dotted lines). The deceleration of the velocity distribution now begins where separation occurred. The shape factor H_2 is moderate but grows towards the trailing edge. Despite the disturbance by the roughness the momentum thickness is by far smaller than behind the bubble resulting in less drag.

Detailed flow field observations were taken in the transition region of a Wortman FX66-196 airfoil at a Reynolds number of $1.5 \cdot 10^6$ and zero angle of attack. At this condition a laminar separation bubble forms on the upper surface between 0.44 and $0.51x/c$. Mean and fluctuation velocity profiles as well as band-pass filtered fluctuation profiles near the most amplified Tollmien-Schlichting frequencies were measured. The results were compared with linear stability calculations and show good agreement.

Figure 11 shows the shape of this bubble and the mean velocity profiles together with the RMS-profiles at four measurement stations. RMS-data are for a frequency range of 1Hz to 5kHz. Spectral data were collected at the maximum of turbulence energy, which belongs to the point of inflection of the mean velocity profile. Amplification of frequencies in the range of the TS-waves was first noticed at Point 1. All stations upstream have identical fluctuation spectra.

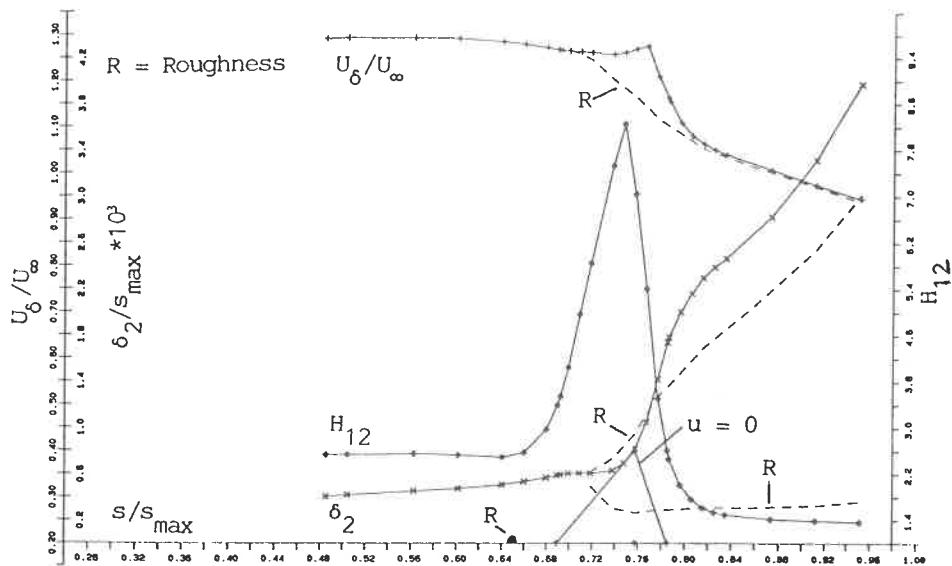


Fig.10: Boundary layer development with and without surface roughness, $Re = 0.7 \cdot 10^5$

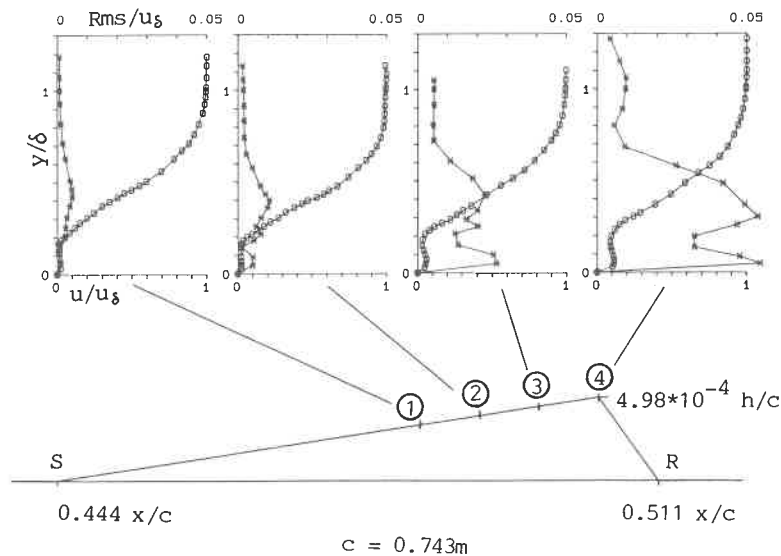


Fig.11: Mean and fluctuation velocity profiles inside a laminar separation bubble with sketch of bubble contour

With a Bruel & Kjaer frequency analyser type 2107 adjusted to an octave selectivity of 40dB band-pass filtered velocity fluctuations were measured through the boundary layer at each station. The filter center frequency was chosen near the most amplified TS-frequency. The result is plotted in Fig.12 to-

gether with the mean velocity profile. The measured points are denoted with symbols. Based on the mean velocity profile stability calculations were performed by direct solution of the Orr-Sommerfeld equation. To achieve convergence of the solver, the measured data points must be carefully splined and interpolated to get a minimum of 100 points. The splined mean velocity distribution and the resulting Eigenfunction of the u-fluctuation are shown as a solid line. The maximum of the Eigenfunction and the measured RMS-data are normalized to 1. Outside the bubble the shape of the Eigenfunction is in good agreement with the measured fluctuation velocity but at the upper edge of the bubble the measurements show an additional maximum. The maximum inside the bubble is overpredicted. The calculated amplification ratio $\alpha_i = \alpha_1 * \delta_1$ for this frequency is -0.22 , close to the measured one of -0.21 .

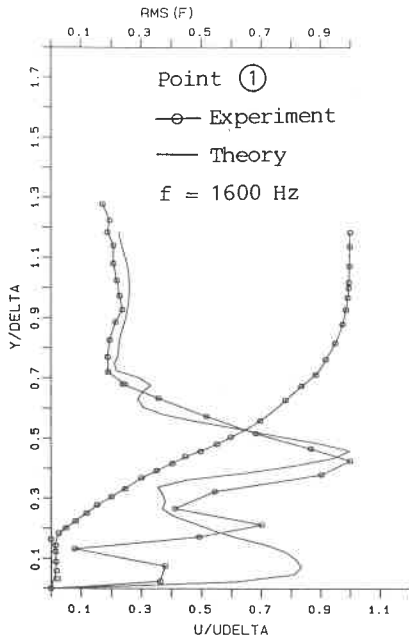


Fig.12: Exp. profile and Eigenfunction of Orr-Sommerfeld DGL

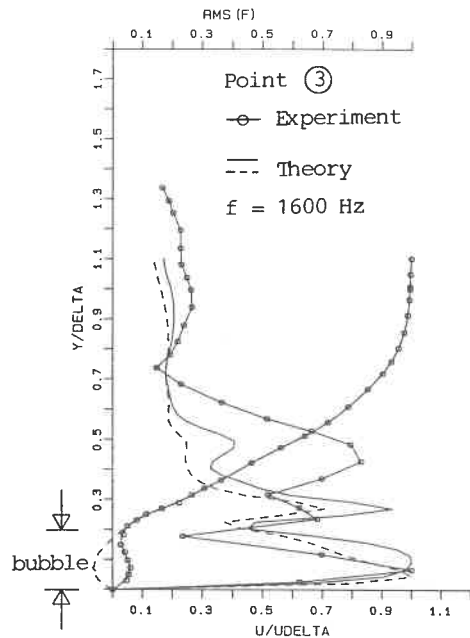


Fig.13: Additional calculation for reversed velocity inside bubble

Figure 13 shows the same comparison for a station (Point 3) only $0.013x/c$ downstream of the first one. This is nearly identical to one wavelength of a TS-wave with 1600Hz as calculated for Point 1. The amplitude measured at the inflection point has grown by a factor of 6.3 . Inside the bubble a small mean velocity component is visible. The Eigenfunction and the u-fluctuation profile show only poor agreement outside the bubble but the first maximum inside the bubble and the second one slightly above the bubble is better predicted than for

Point 1. To examine the influence of the mean velocity direction, the velocity data inside the bubble were rectified and the calculations performed again. The result is also plotted in Fig. 13 as a dashed line. The shape of the Eigenfunction shows only astonishing small differences from the first one. The amplification ratio α_i calculated for the original profile is -0.26 , with reversed velocity -0.32 . The measured α_i begins to decrease and reaches only -0.15 .

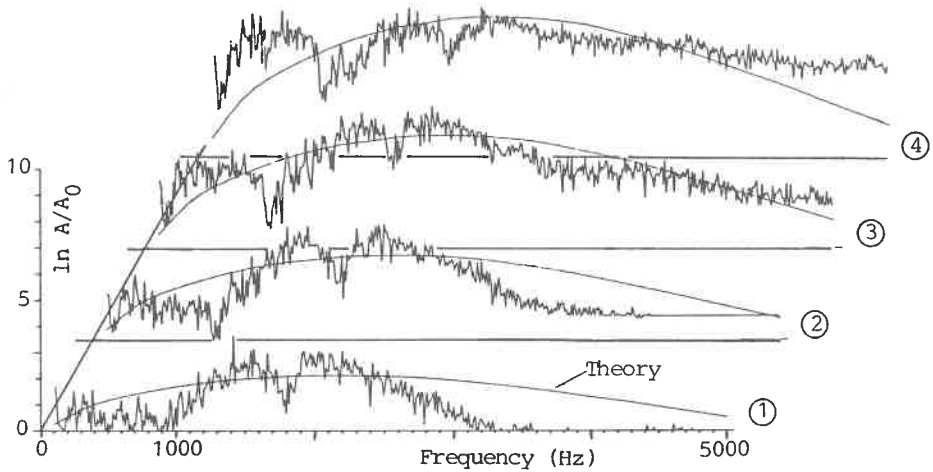


Fig.14: Comparison of amplitudes related to station $0.471 x/c$

Fig. 14 shows an overall comparison of amplitude spektra. Measured and calculated amplitudes are related to the amplitudes at the last station upstream of Point 1. For clearness the zero-point is offset at each station and marked by a horizontal line. The growth of amplitudes in this region is well predicted by linear stability theory. It is remarkable that the maximum amplitude ratio $\ln A/A_0=n$, which can be measured reaches only $n=6$. This problem is also observed by other experimentators [6]. It can be illustrated by plotting the measured spectral energy for a finite frequency range together with the expected spectral energy calculated upstream from transition using theoretical α_i . Fig.15 shows that the measured spectral energy levels out upstream of Point 1, whereas the calculations predict smaller amplitudes. Measurements outside the boundary layer show that the noise level of the hotwire anemometry is about a factor of 10 smaller than the smallest observed amplitude inside the boundary layer. An explanation for this problem is not found yet.

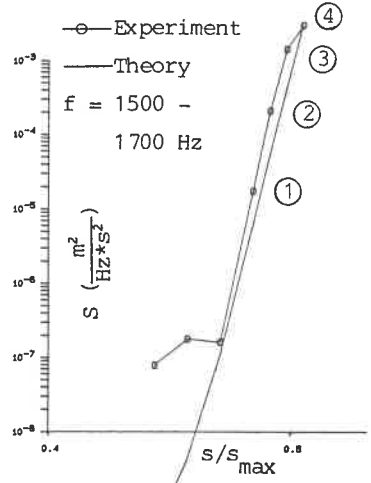


Fig.15: Energy spectrum extrapolated upstream

CONCLUSIONS

In the present paper only a short survey of the experimental work done in the past is conveyed. A lot of data have been gathered and compared with many existing empirical relations and bubble models [7]. It proves difficult to find correlations which conform with the different data sets. Evaluation is going on and additional experiments are needed.

ACKNOWLEDGEMENTS

This research was supported by the Deutsche Forschungsgemeinschaft under Grant AL242/1-3 and by the Institut für Aerodynamik und Gasdynamik der Universität Stuttgart.

REFERENCES

- [1] F.X.Wortmann and D.Althaus:Der Laminarwindkanal des Instituts für Aerodynamik und Gasdynamik der Technischen Hochschule Stuttgart.
- [2] E.Dobbinga,J.L. van Ingen and J.W.Kooi: Some research on two dimensional laminar separation bubbles. AGARD-CPP-102,1972.
- [3] C.Y.Liu and V.A.Sandborn:Evaluation of the sepatation properties of laminar boundary layers.The Aeronautical Quarterly, Aug.1968, Vol.XIX.
- [4] Green J.E.:Two dimensional turbulent reattachment as a boundary-layer problem.AGARD CP4,Pt.I,1966.
- [5] E.J.Fitzgerald and Th.J.Mueller:Measurements in a separation bubble on an airfoil using Laser Velocimetry. AIAA Journal, Vol.28, Nr.14,1990.
- [6] LeBlanc,P.,Blackwelder,R.,Liebeck,R.
A Comparison between Boundary Layer Measurements in a Laminar Separation Bubble Flow and Linear Stability Theory Calculations.
Department of Aerospace Engineering
University of Southern California.
- [7] D.Althaus,W.Würz:Schlußbericht für die Deutsche Forschungsgemeinschaft über das Forschungsvorhaben: Experimentelle Untersuchung laminarer Ablöseblasen. Institutsbericht (1988).